Electronic Supplementary Information

For the

Manuscript Entitled

Lanthanide-based coordination polymers as the promising heterogeneous catalysts for ring-opening reactions

Gulshan Kumar, Girijesh Kumar, and Rajeev Gupta*

Department of Chemistry, University of Delhi

Delhi – 110 007, India

List of Figures:

List of Tables:

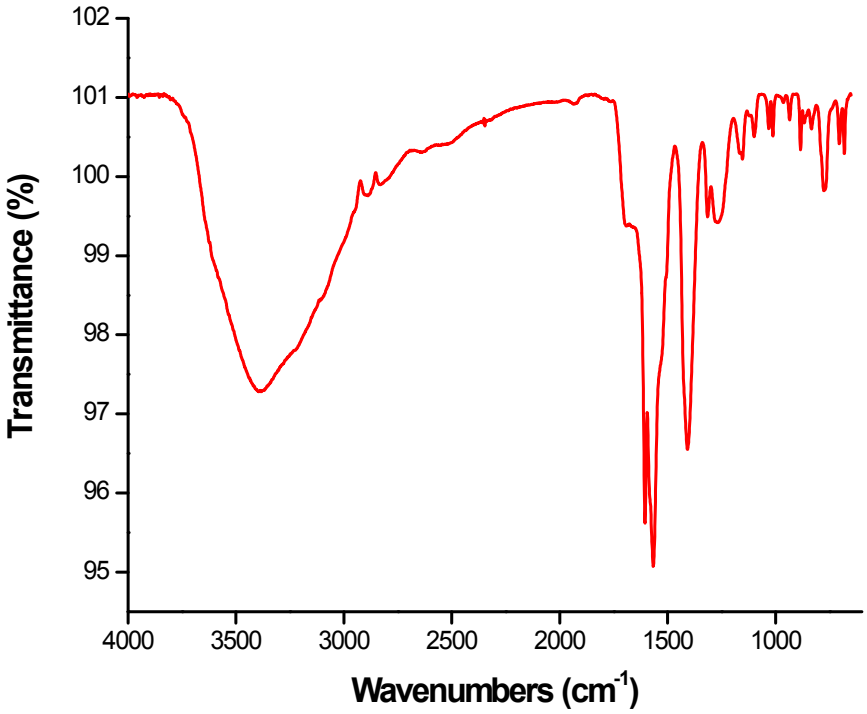

Figure S1. FTIR spectrum of **1-Eu**.

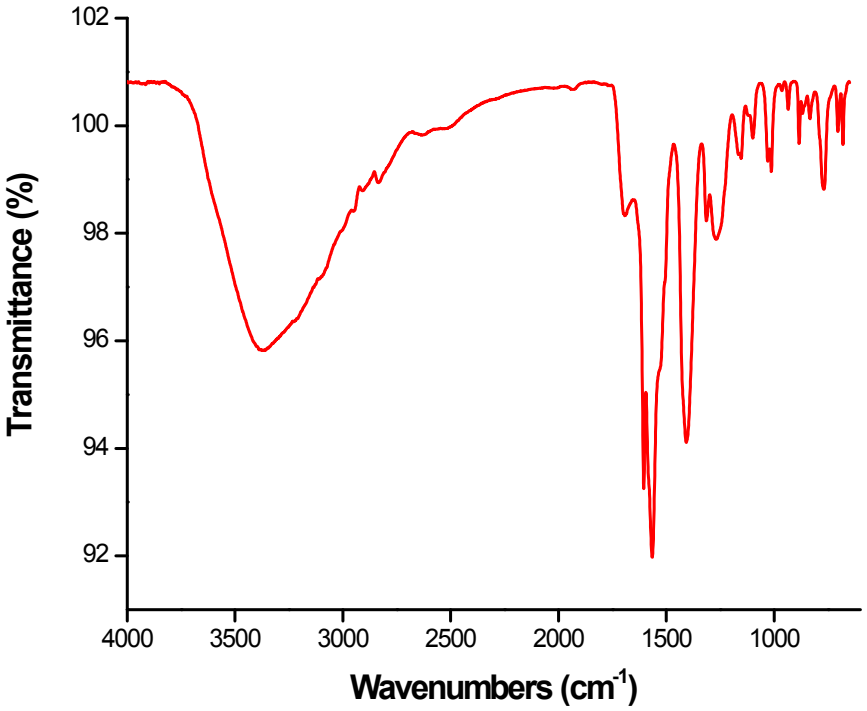

Figure S2. FTIR spectrum of **1-Tb**.

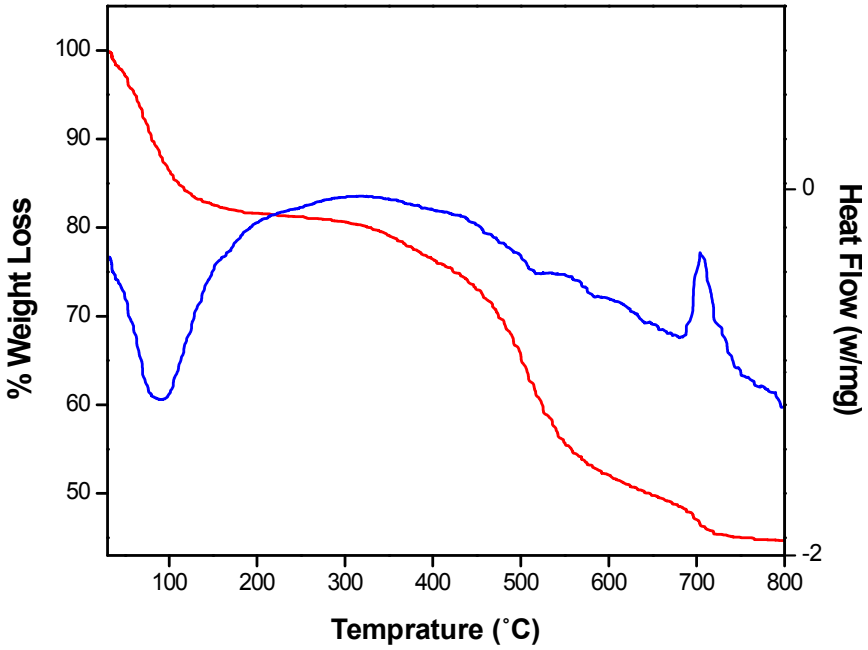

Figure S3. Thermal Gravimetric Analysis (TGA, red trace) and Differential Scanning Calorimetric (DSC, blue trace) plots for **1-Eu**.

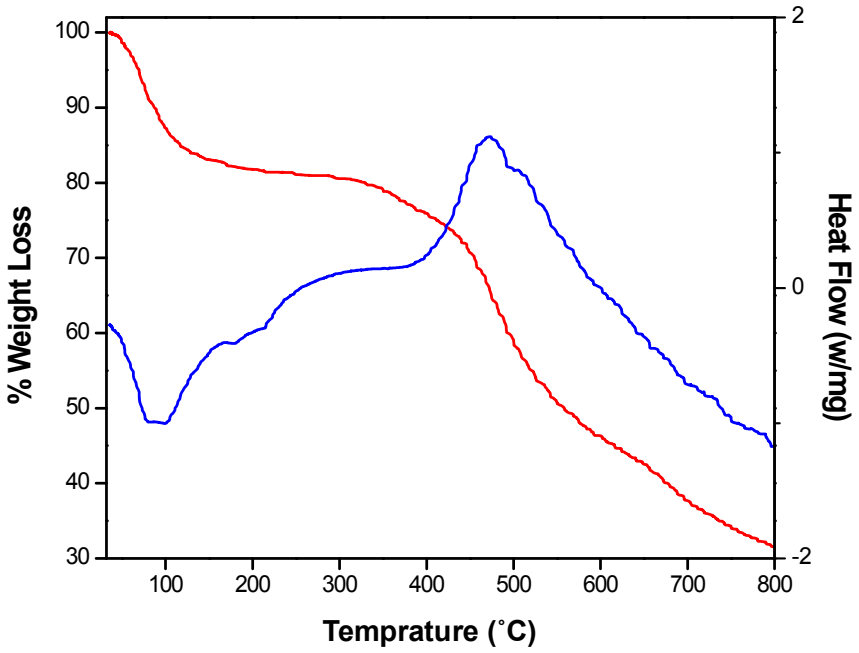

Figure S4. Thermal Gravimetric Analysis (TGA, red trace) and Differential Scanning Calorimetric (DSC, blue trace) plots for **1-Tb**.

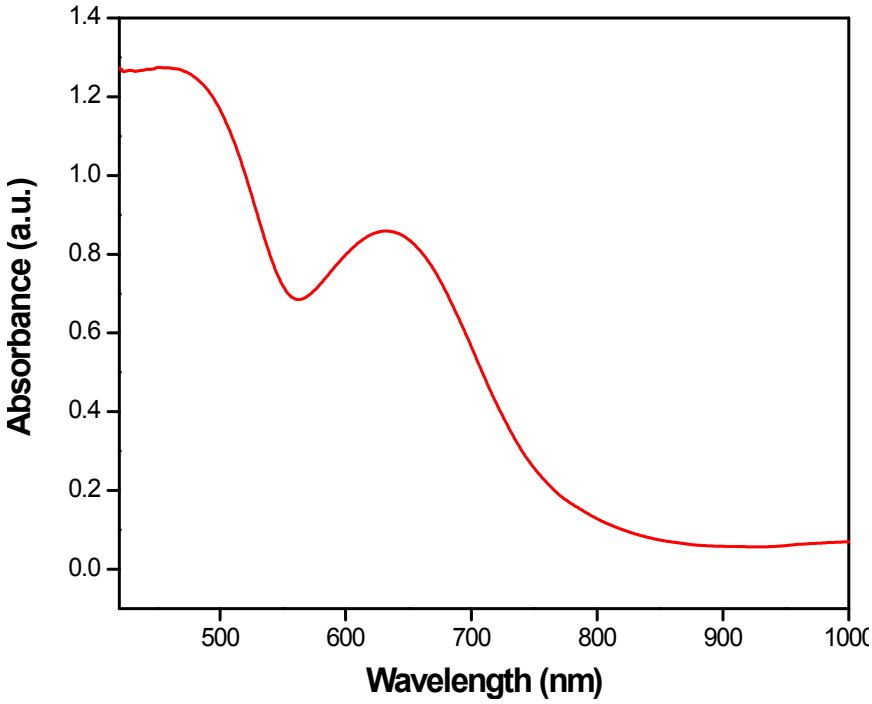

Figure S5. Diffuse reflectance UV-Vis spectrum of **1-Eu**.

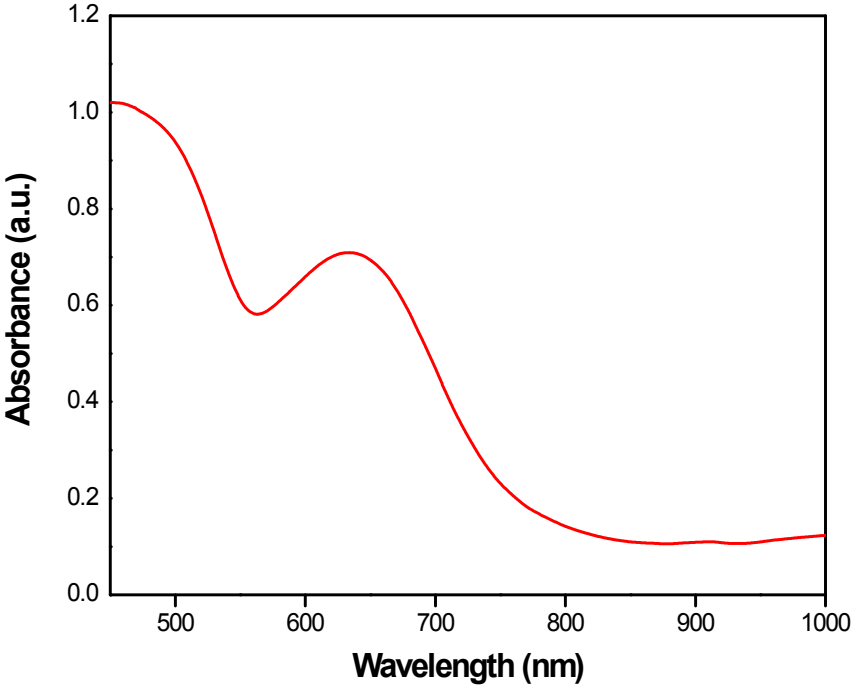

Figure S6. Diffuse reflectance UV-Vis spectrum of **1-Tb**.

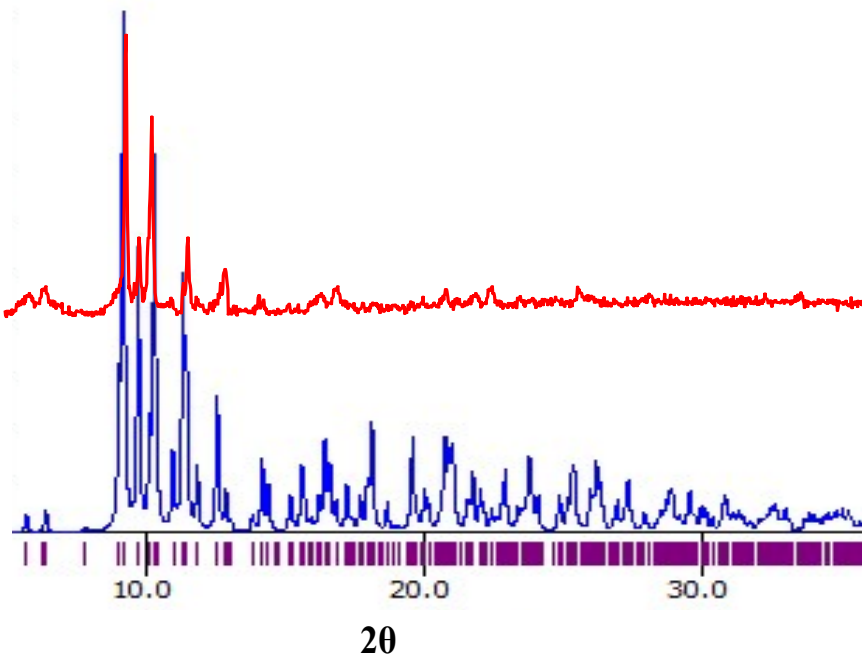

Figure S7. X-ray Powder Diffraction (XRPD) pattern for as synthesized **1-Eu** (red trace) and the one simulated from the Mercury 3.0 using single crystal data (blue trace).

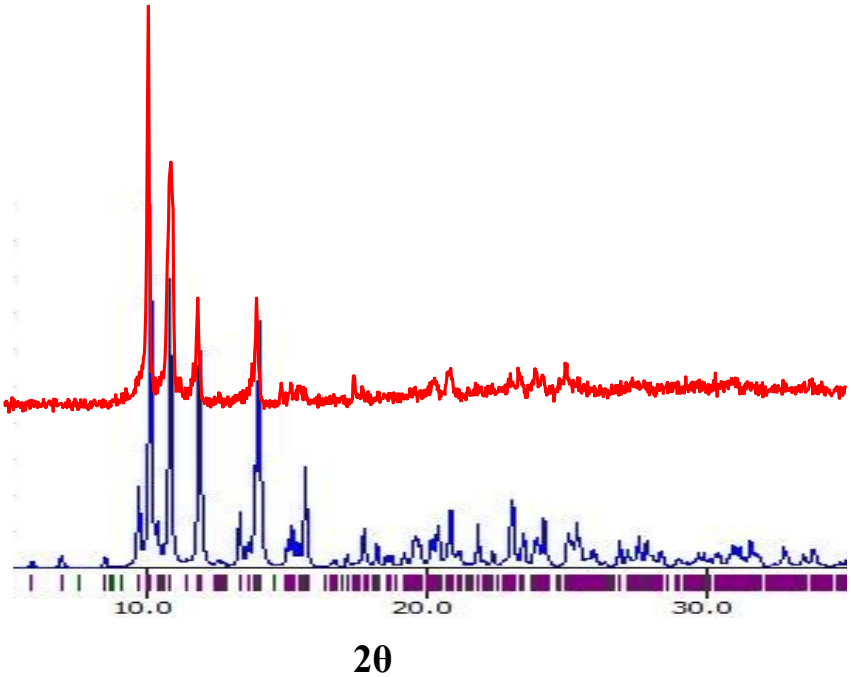

Figure S8. X-ray Powder Diffraction (XRPD) pattern for as synthesized **1-Tb** (red trace) and the one simulated from the Mercury 3.0 using single crystal data (blue trace).

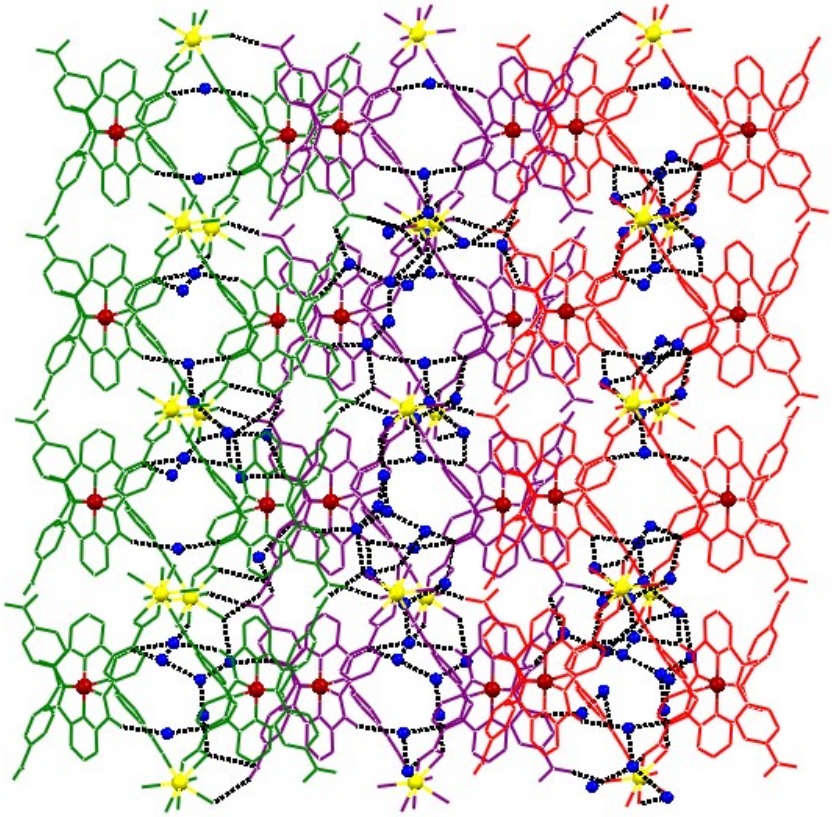

Figure S9. A view of 2D network created due to various hydrogen bonding interactions involving free arylcarboxylic acid groups, O_{amide} groups, and coordinated as well as lattice water molecules connecting various 1D chains (shown in green, magenta, and red colours) in the crystal structure of **1-Tb**.

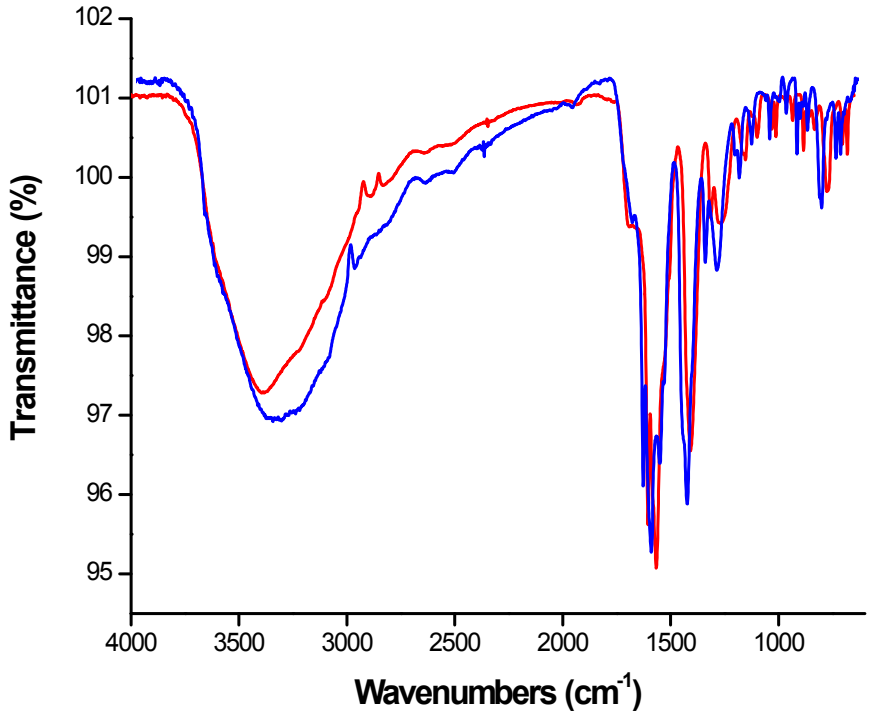

Figure S10. FTIR spectra of as synthesized **1-Eu** (red trace) and after catalysis (blue trace).

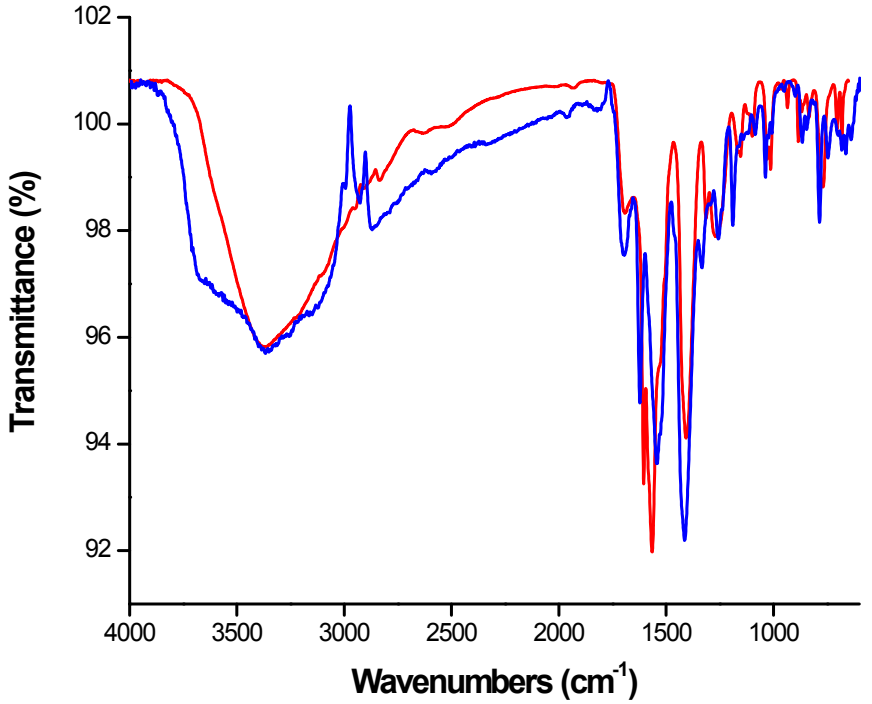

Figure S11. FTIR spectra of as synthesized **1-Tb** (red trace) and after catalysis (blue trace).

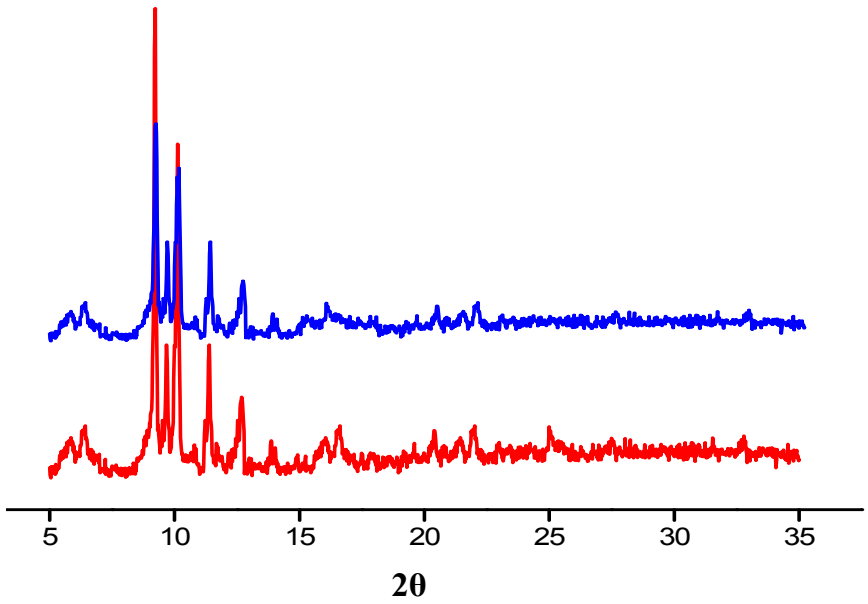

Figure S12. X-ray Powder Diffraction (XRPD) pattern for as synthesized **1-Eu** before (red Trace) and after (blue trace) the ROR between styrene oxide and aniline.

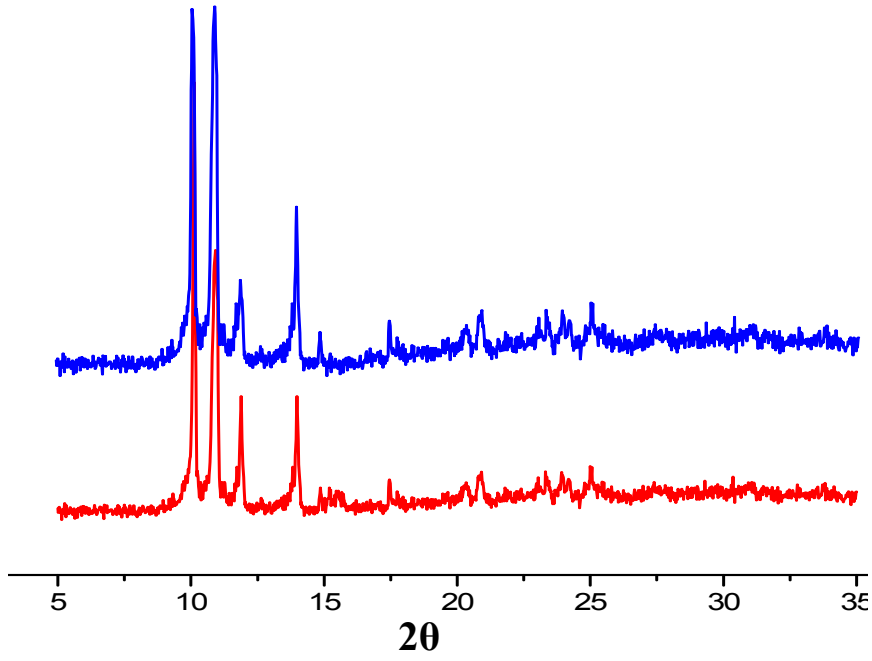

Figure S13. X-ray Powder Diffraction (XRPD) pattern for as synthesized **1-Tb** before (red Trace) and after (blue trace) the ROR between styrene oxide and aniline.

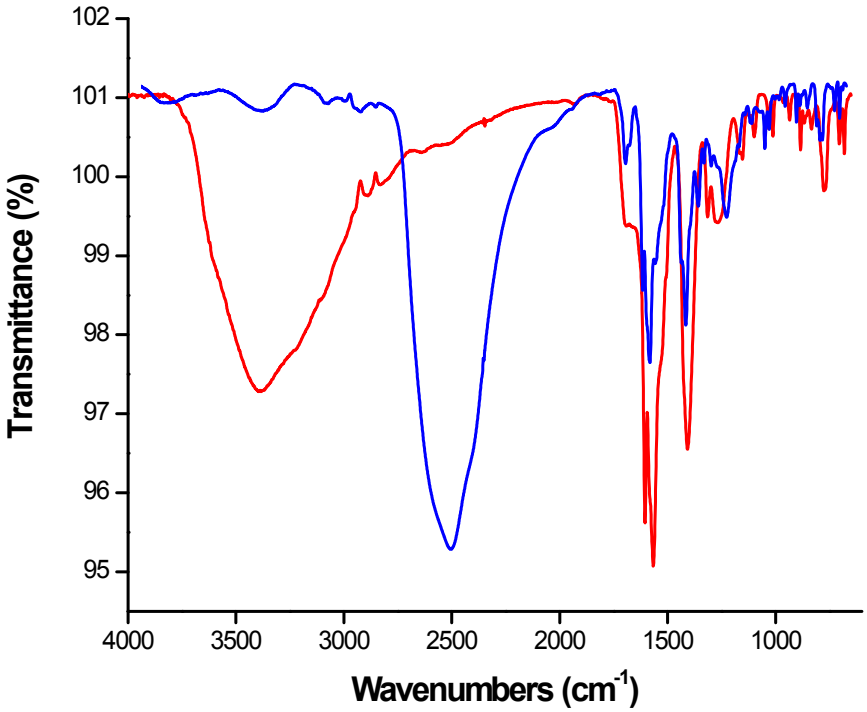

Figure S14. FTIR spectra of as-synthesized **1-Eu** (red trace) and after D_2O exchange experiment (blue trace).

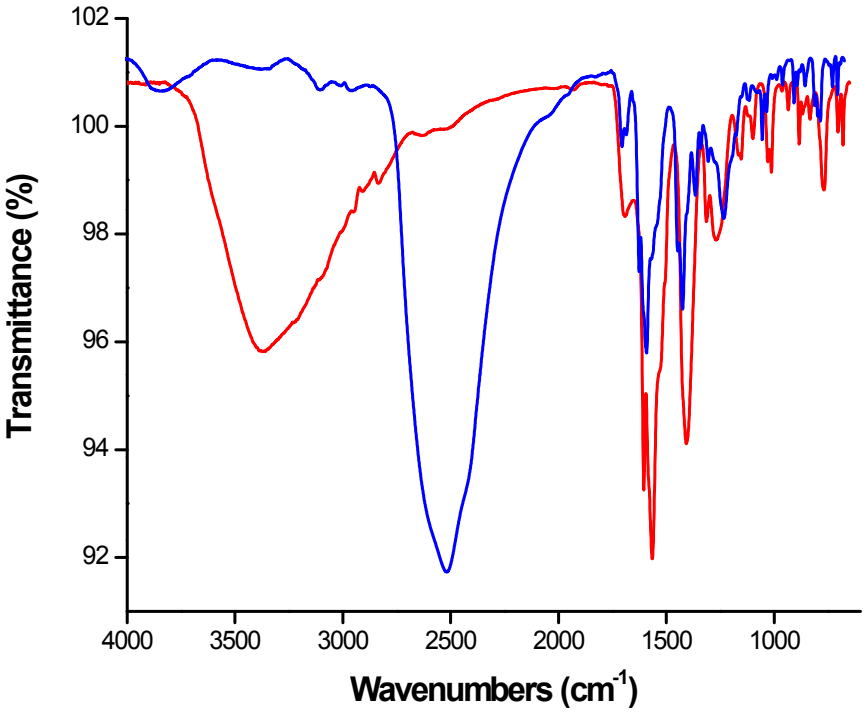

Figure S15. FTIR spectra of as-synthesized **1-Tb** (red trace) and after D_2O exchange experiment (blue trace).

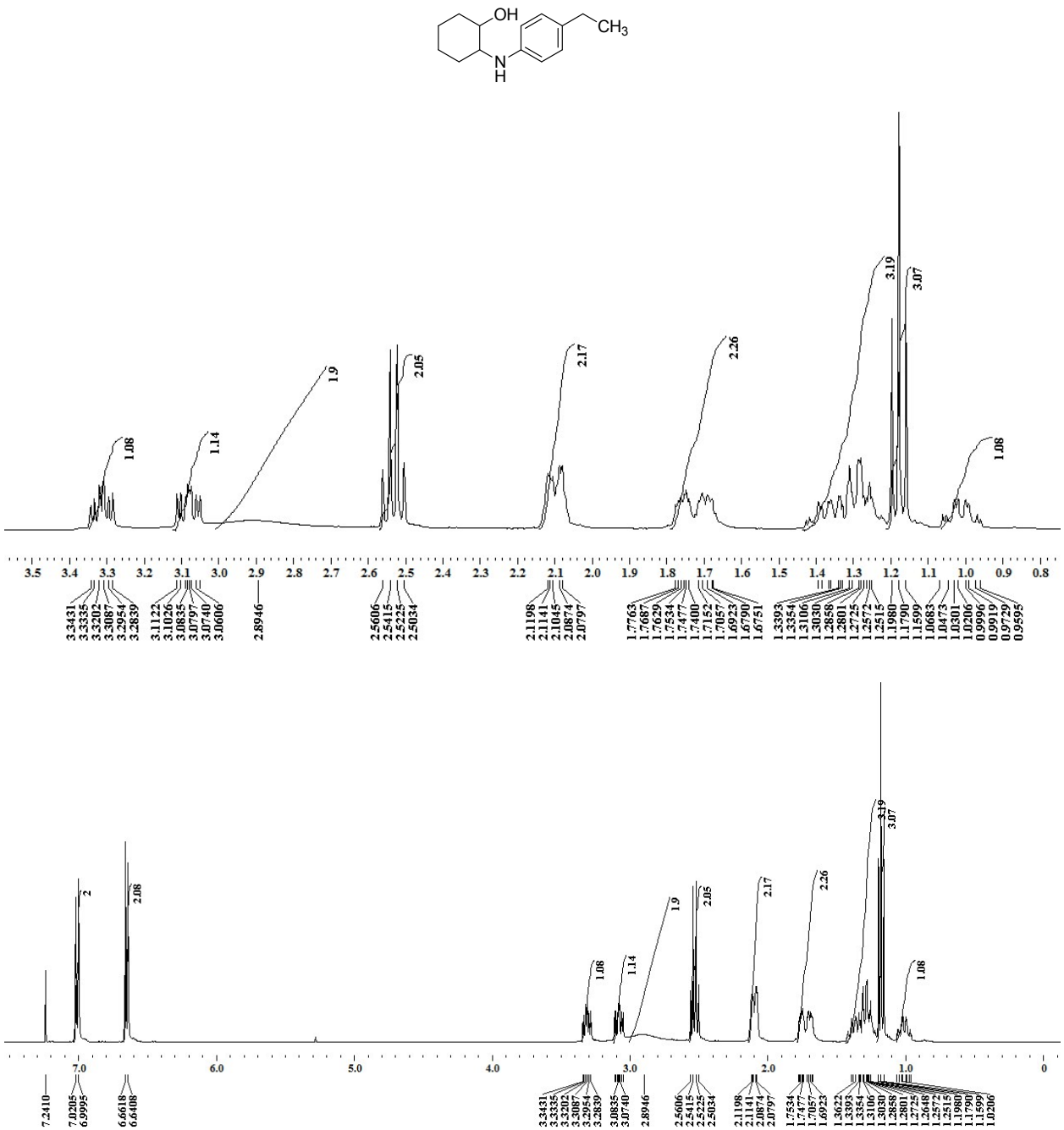

Figure S16. ^{1}H NMR spectrum of 2-((4-Ethylphenyl)amino)cyclohexanol in $CDCl_3$.

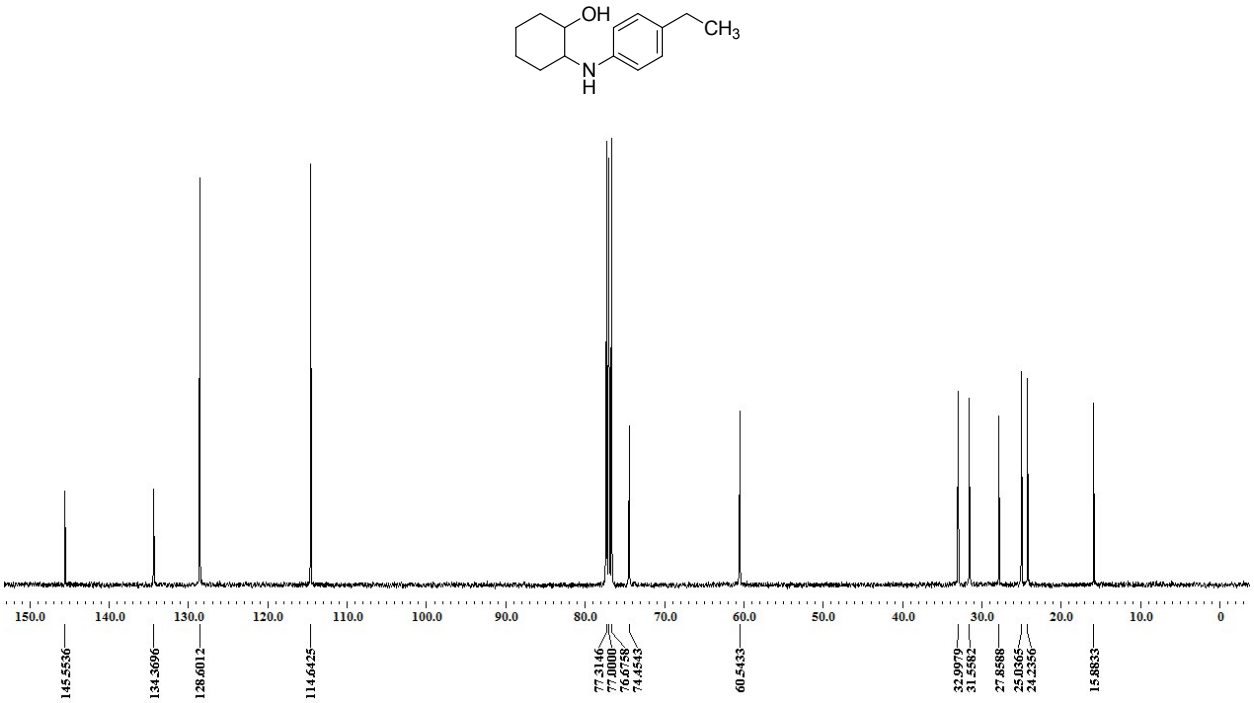

Figure S17. ^{13}C NMR spectrum of 2-((4-Ethylphenyl)amino)cyclohexanol in $CDCl_3$.

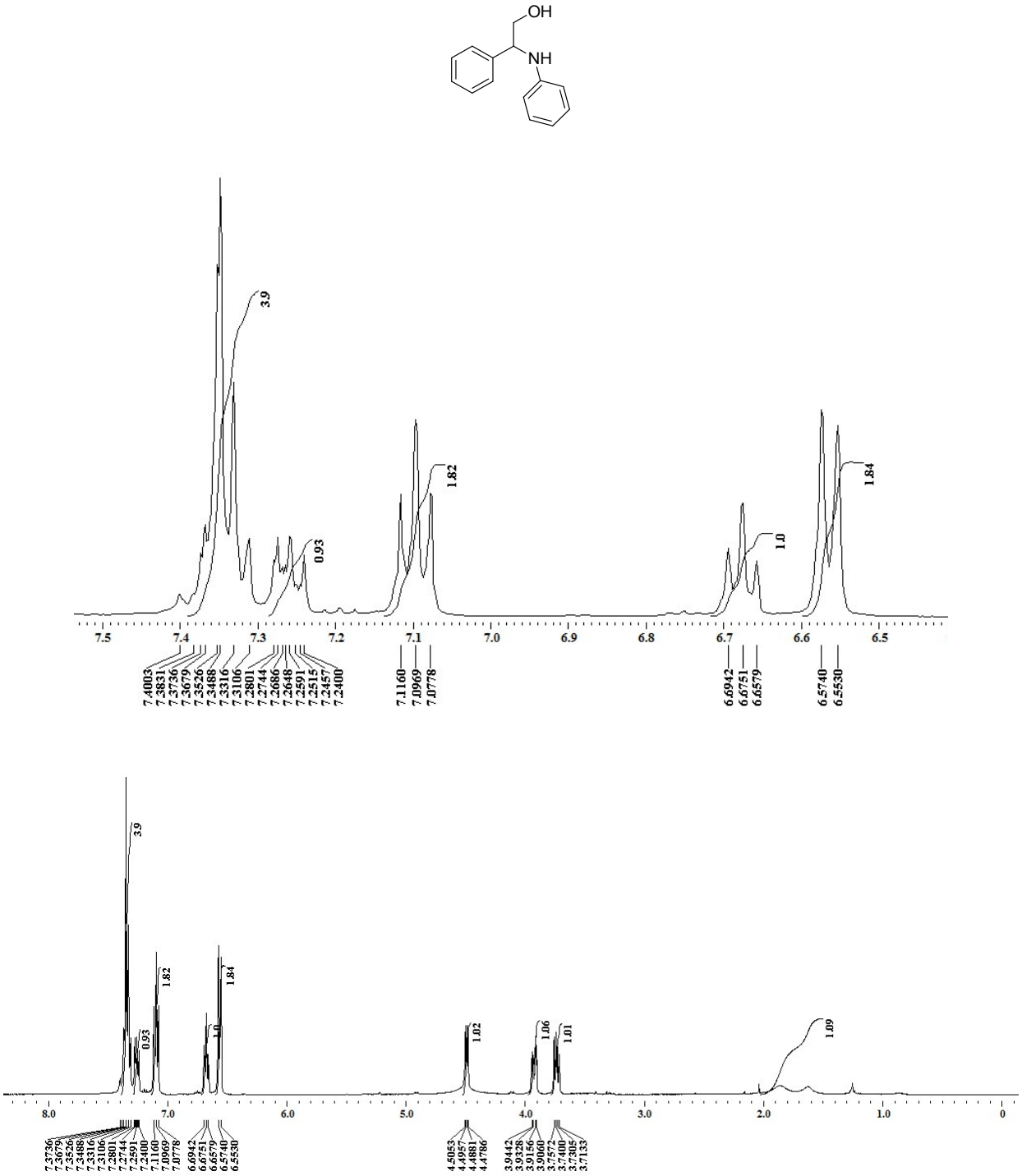

Figure S18. ^{1}H NMR spectrum of 2-Phenyl-2-(phenylamino)ethanol in $CDCl_3$.

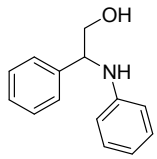

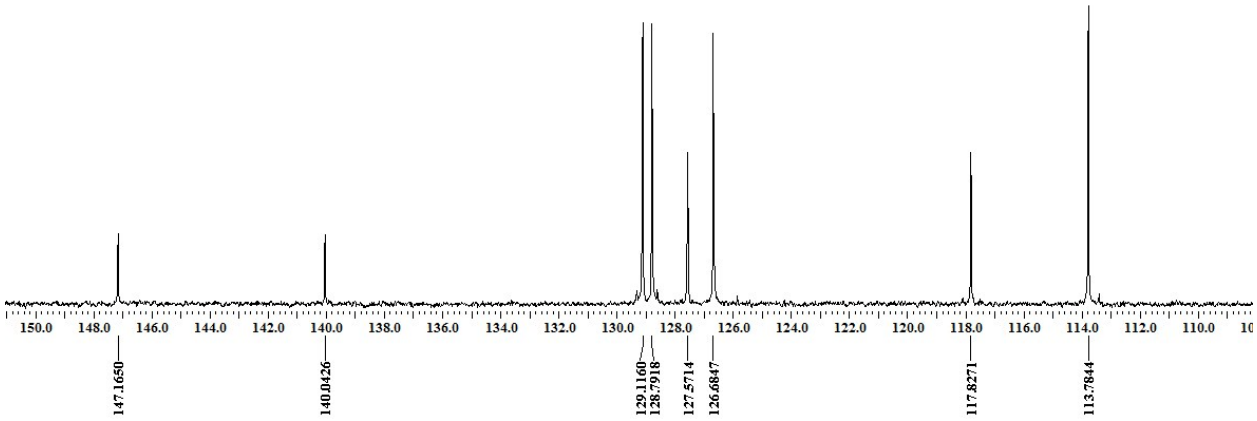

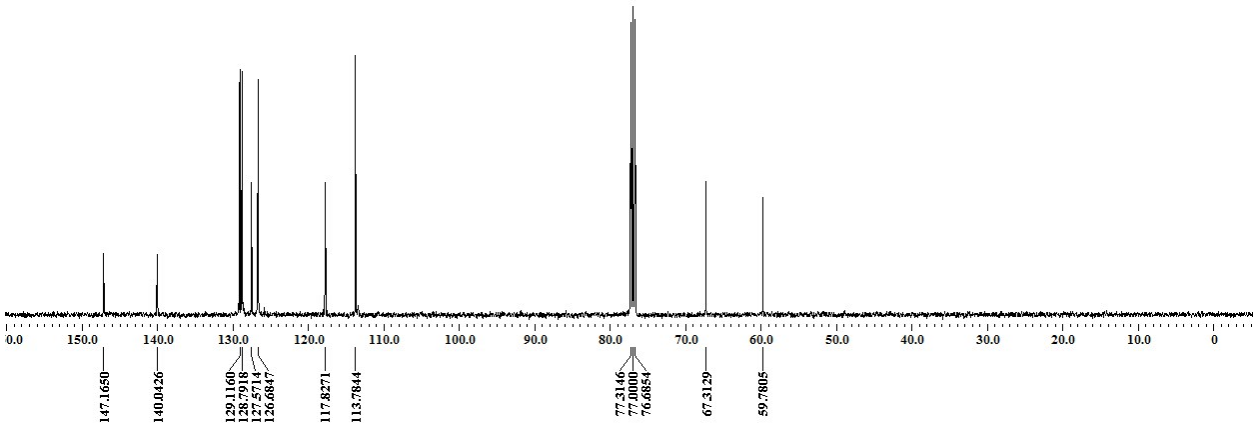

Figure S19. ^{13}C NMR spectrum of 2-Phenyl-2-(phenylamino)ethanol in $CDCl_3$.

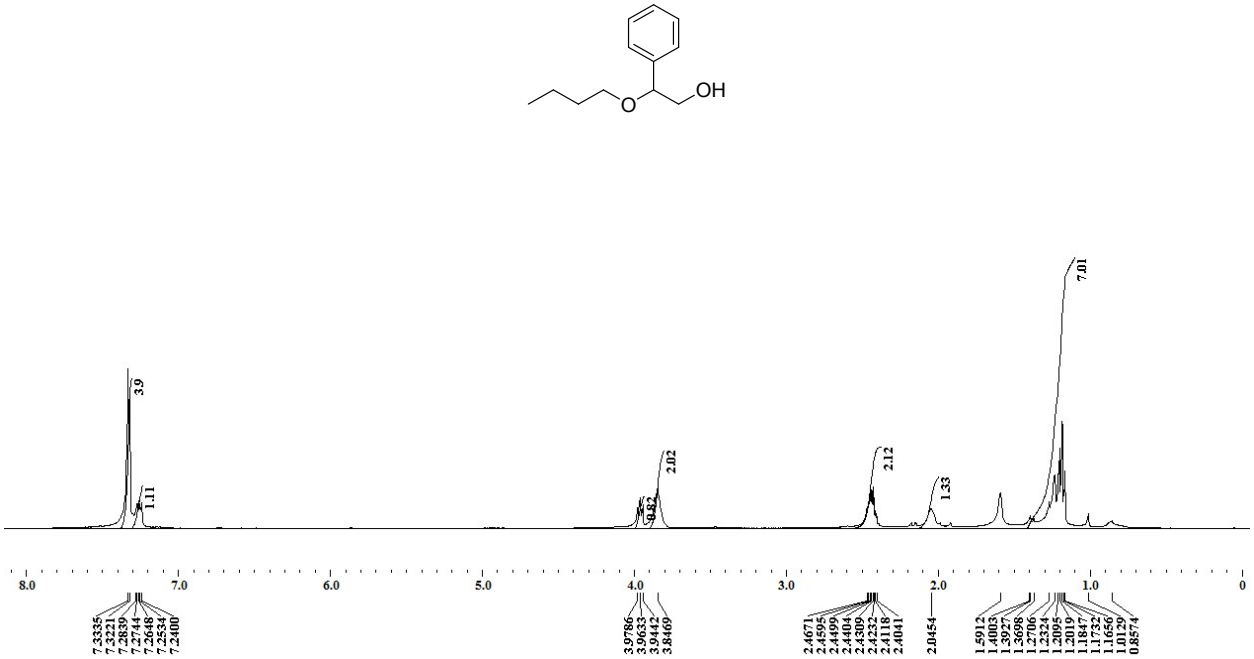

Figure S20. ^{1}H NMR spectrum of 2-Butoxy-2-phenylethanol in $CDCl_3$.

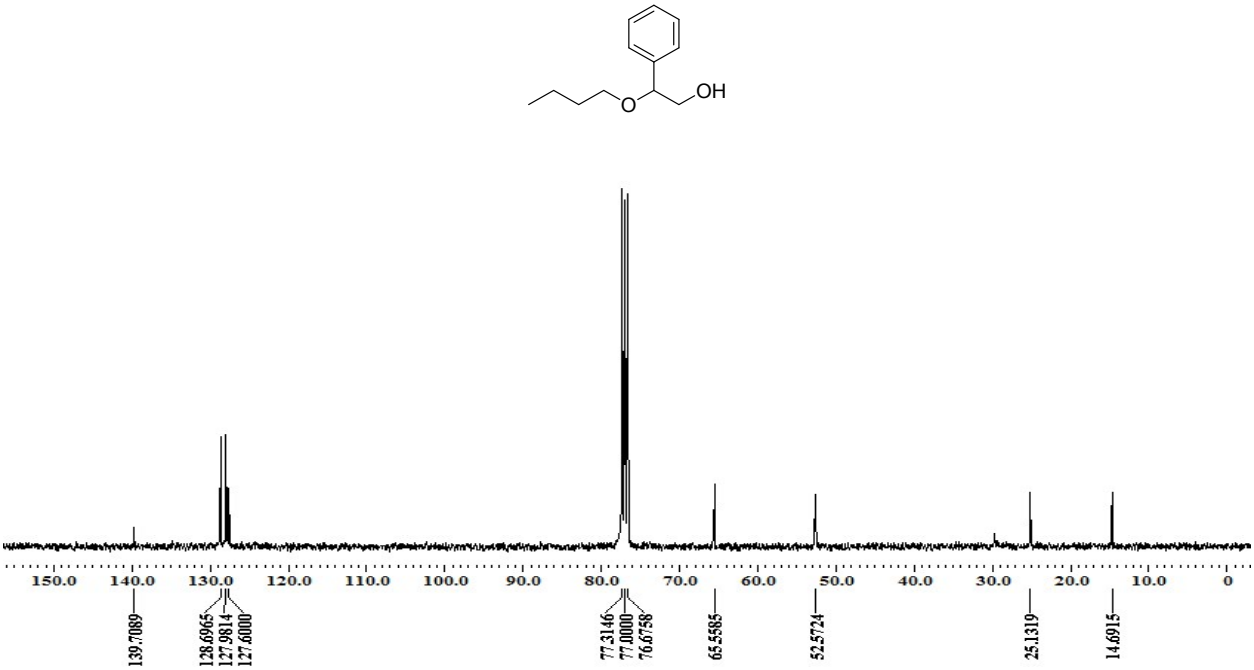

Figure S21. ^{13}C NMR spectrum of 2-butoxy-2-phenylethanol in $CDCl_3$.

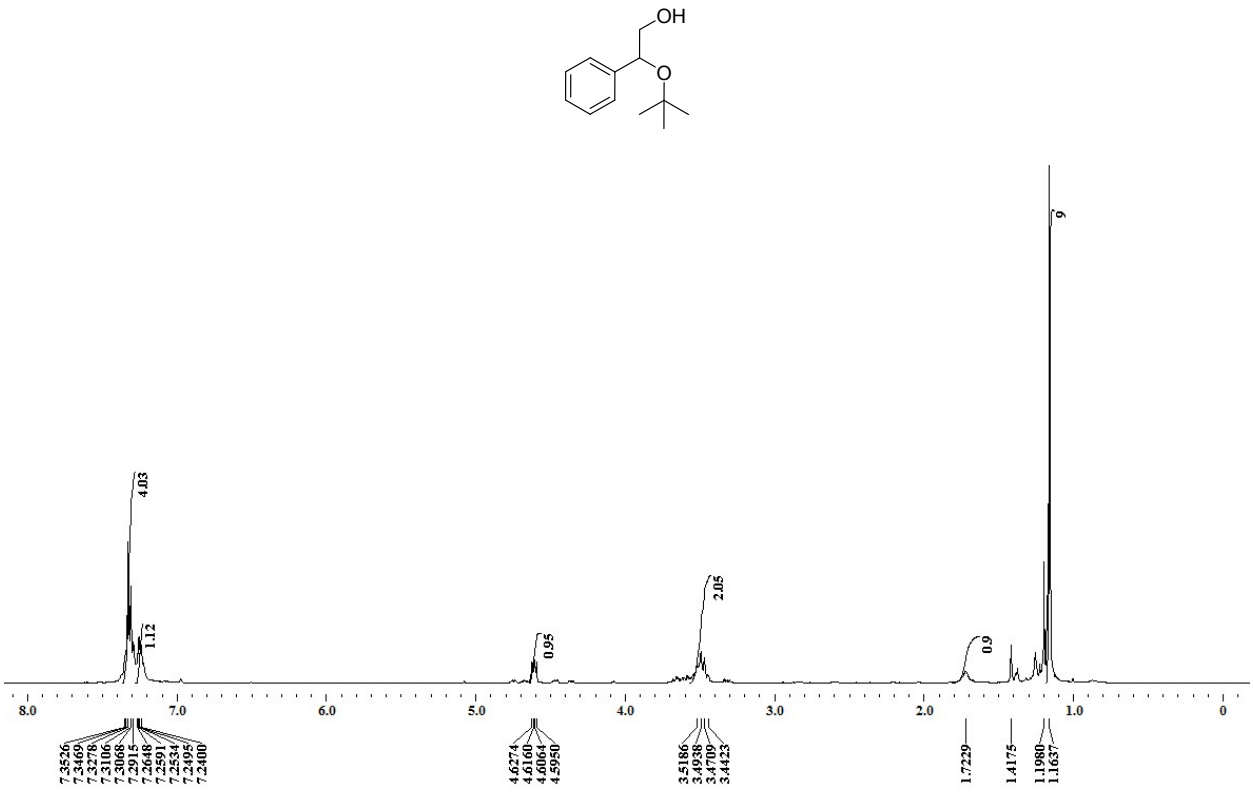

Figure S22. ^{1}H NMR spectrum of 2-(tert-Butoxy)-2-phenylethanol in $CDCl_3$.

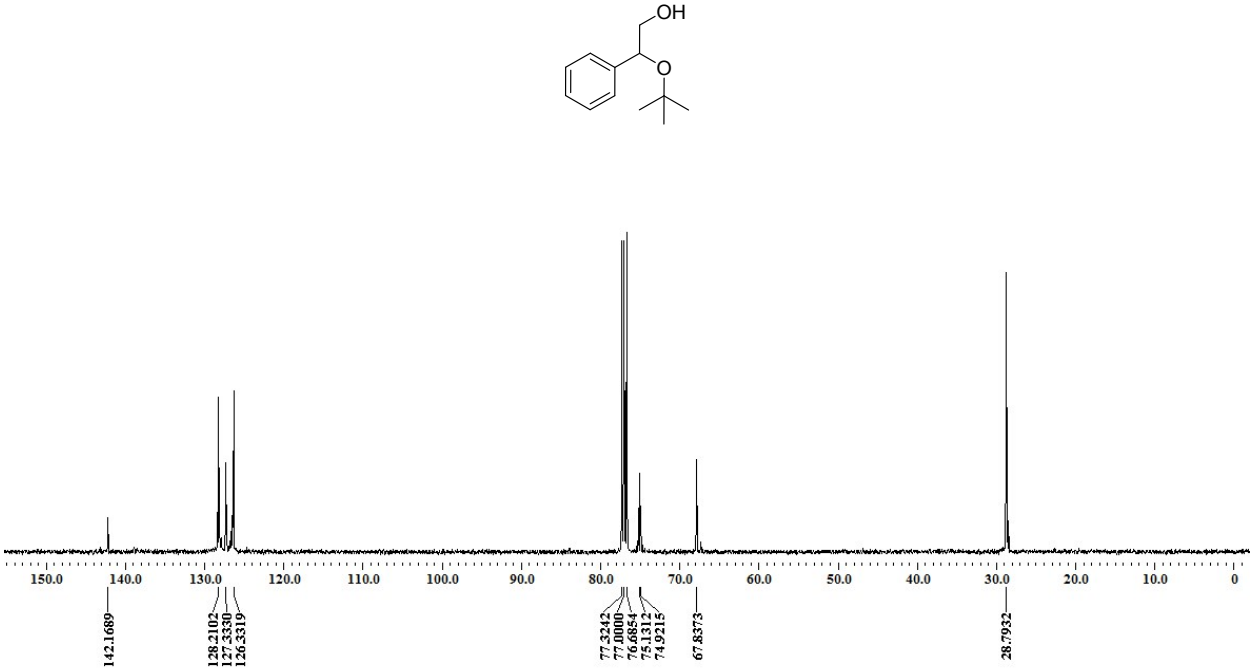

Figure S23. ^{13}C NMR spectrum of 2-(tert-Butoxy)-2-phenylethanol in $CDCl_3$.

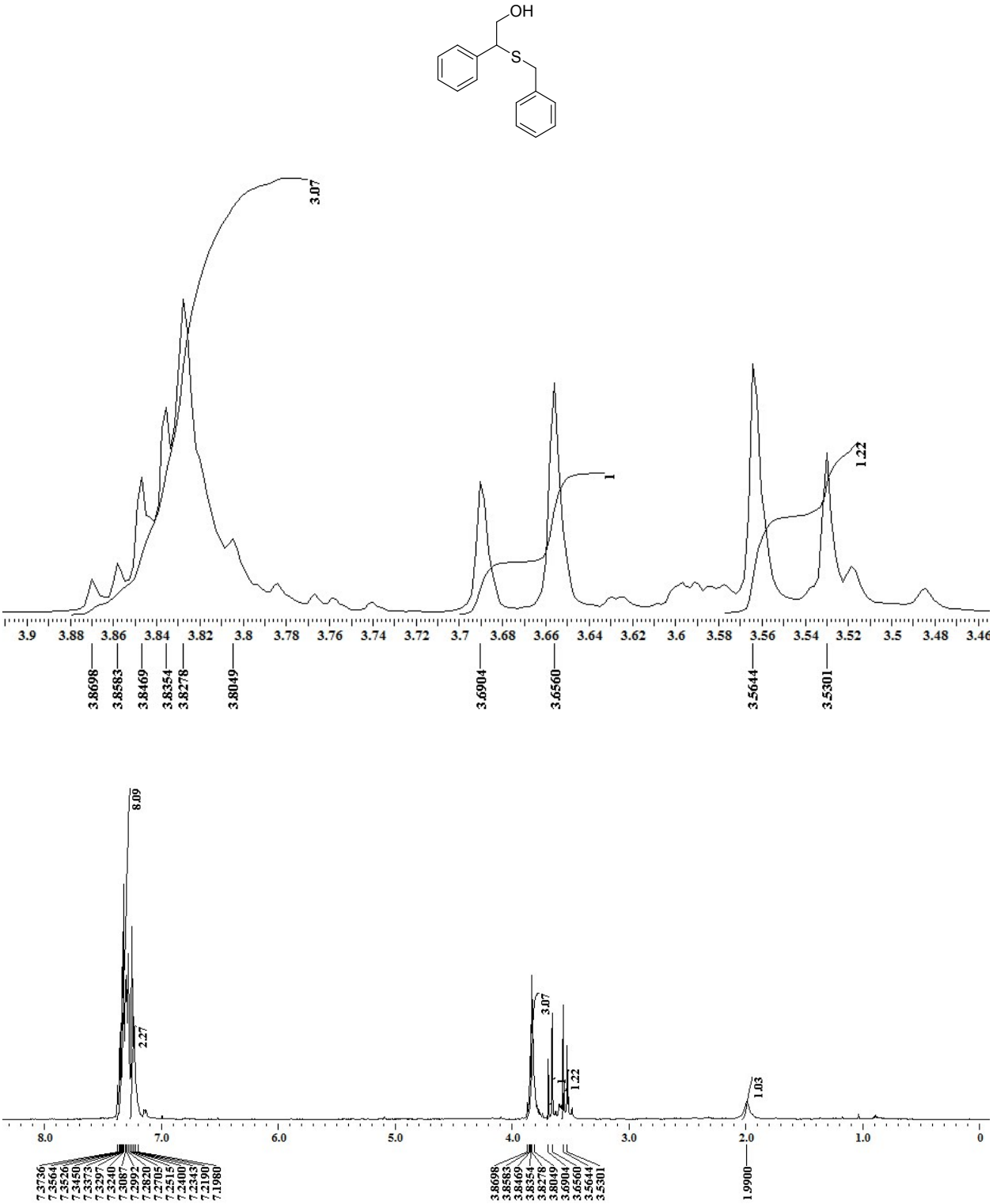

Figure S24. ^{1}H NMR spectrum of 2-(Benzylthio)-2-phenylethanol in $CDCl_3$.

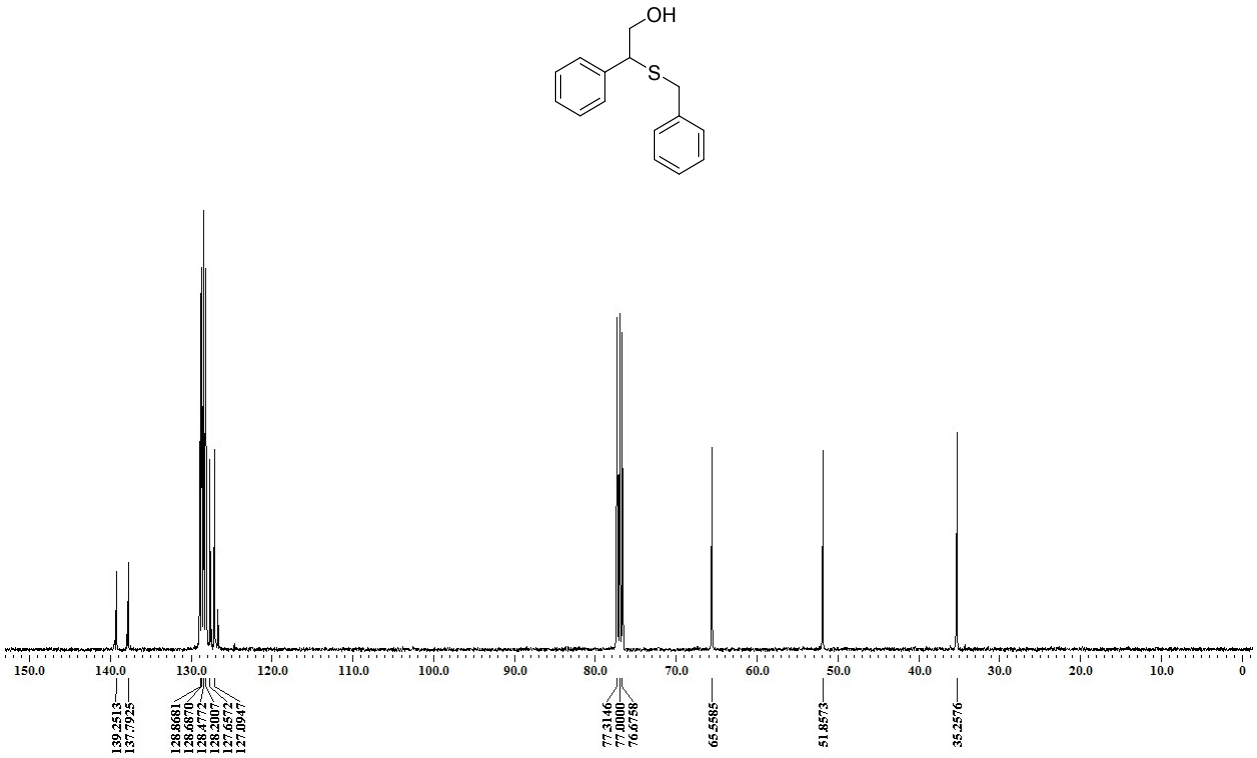

Figure S25. ^{13}C NMR spectrum of 2-(Benzylthio)-2-phenylethanol in $CDCl_3$.

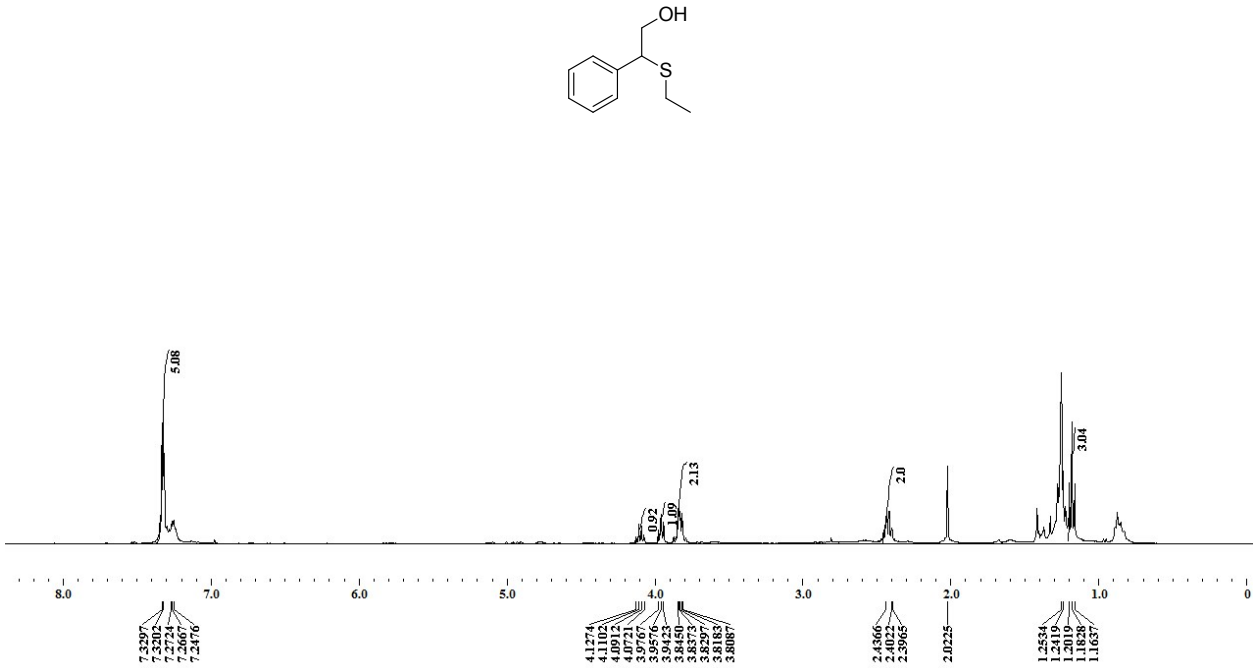

Figure S26. ^{1}H NMR spectrum of 2-(Ethylthio)-2-phenylethanol in $CDCl_3$.

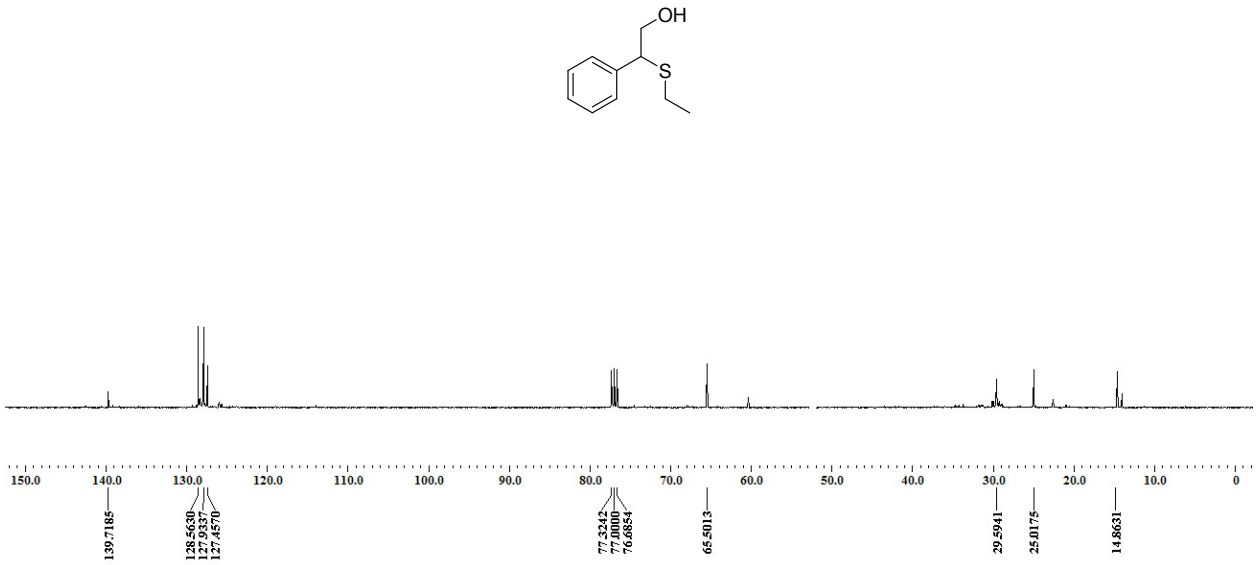

Figure S27. ^{13}C NMR spectrum of 2-(Ethylthio)-2-phenylethanol in $CDCl_3$.

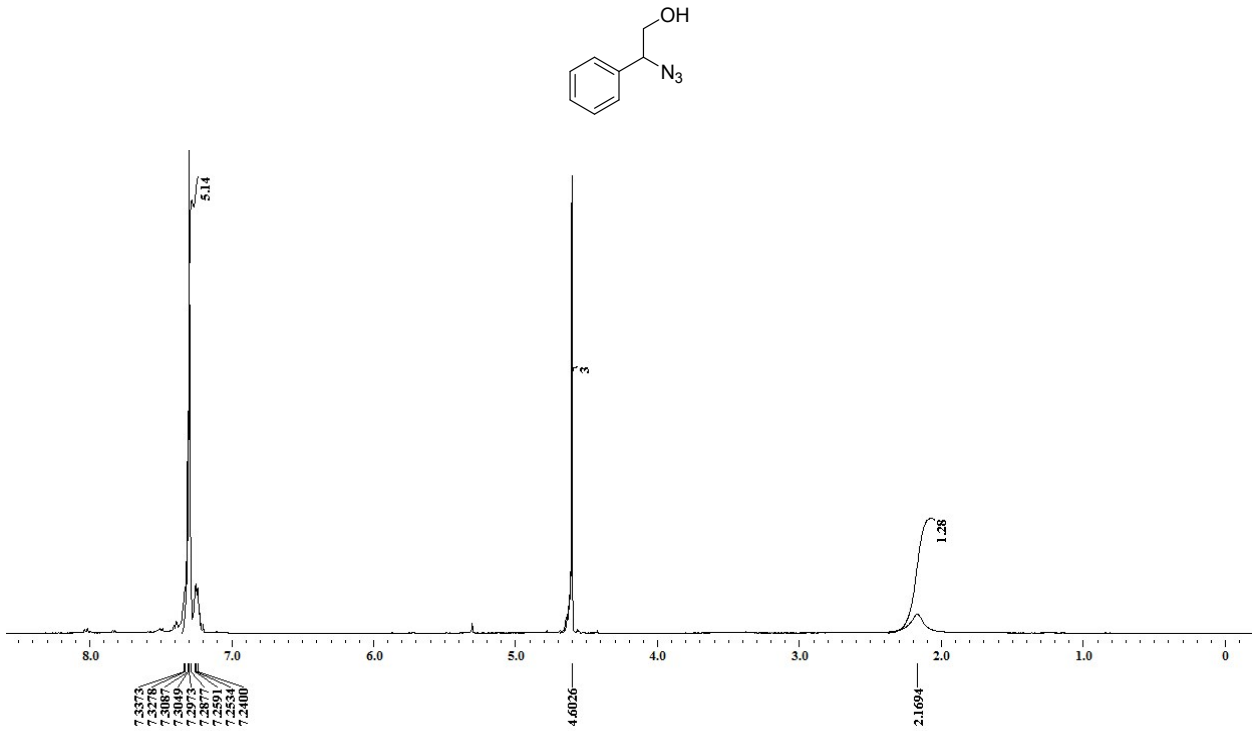

Figure S28. ^{1}H NMR spectrum of 2-Azido-2-phenylethanol in $CDCl_3$.

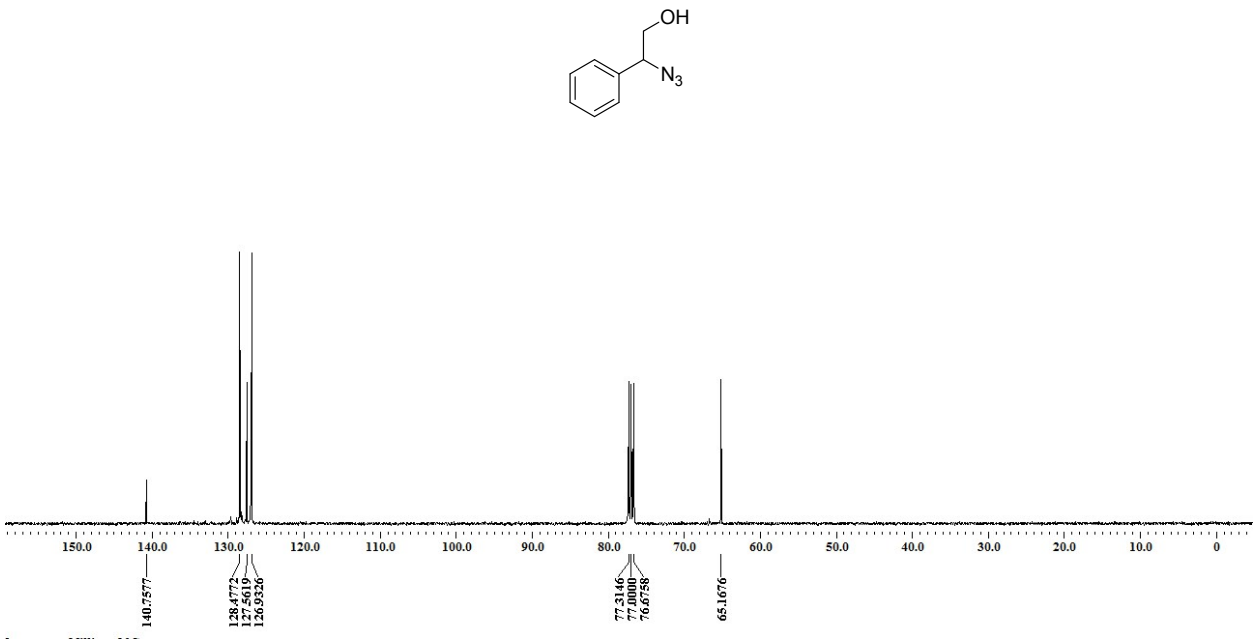

Figure S29. ^{13}C NMR spectrum of 2-Azido-2-phenylethanol in $CDCl_3$.

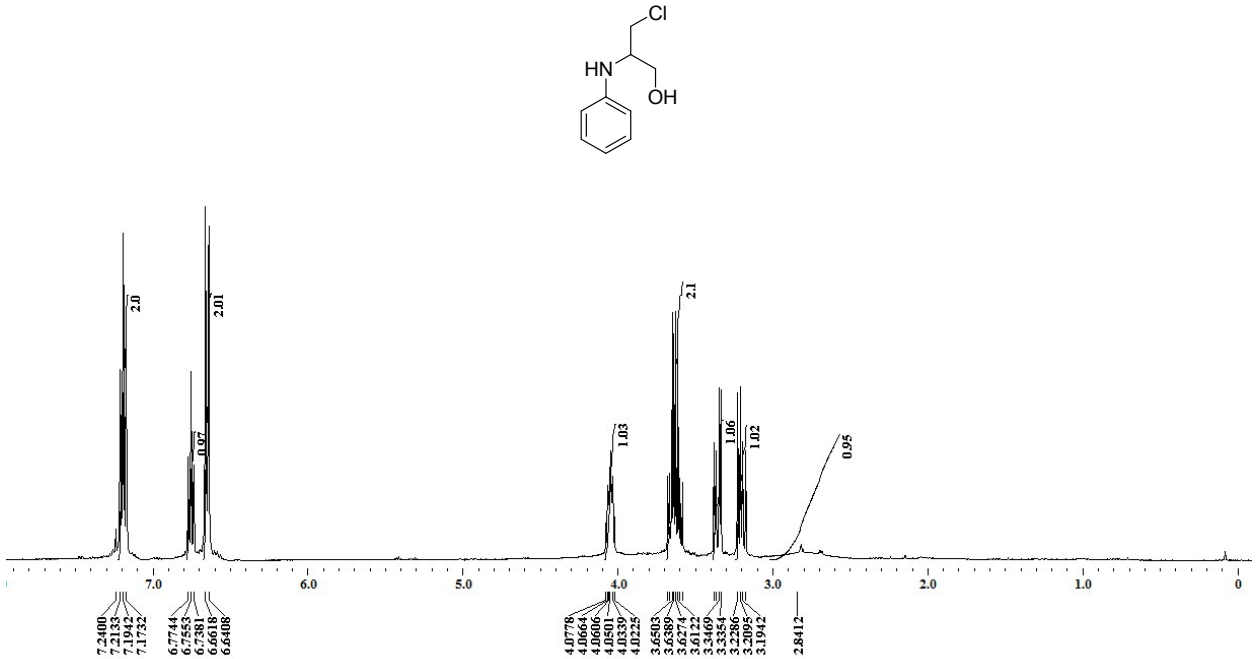

Figure S30. ^{1}H NMR spectrum of 3-Chloro-2-(phenylamino)propan-1-ol in $CDCl_3$.

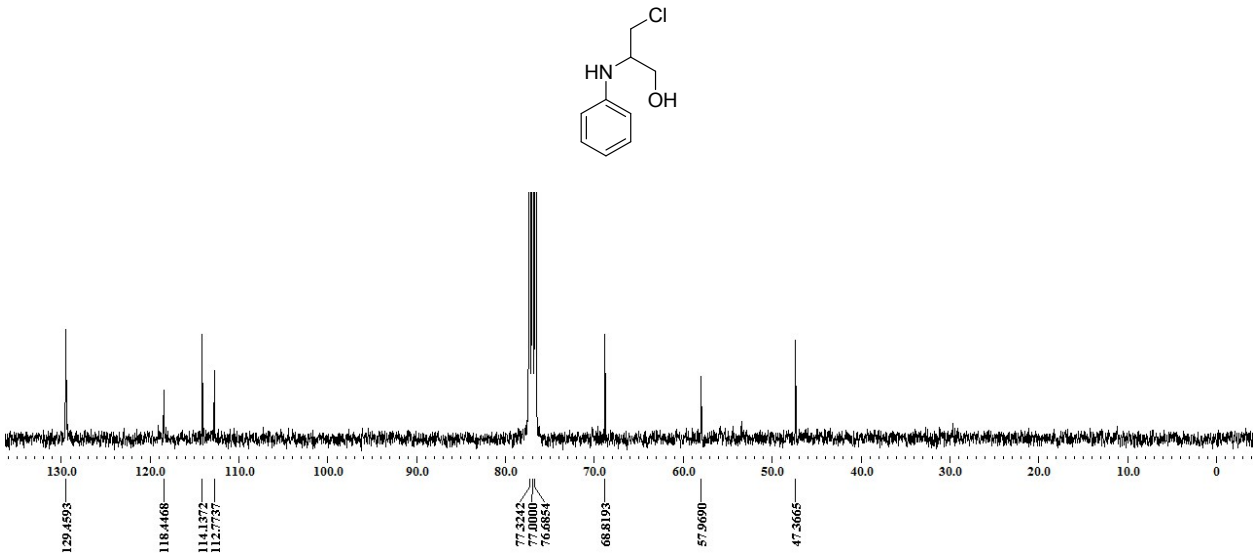

Figure S31. ^{13}C NMR spectrum of 3-Chloro-2-(phenylamino)propan-1-ol in $CDCl_3$.

Table S1. H-bonding distances for **1-Eu**.

Hydrogen bonding synthon	**Separation (Å)**	**Hydrogen bonding synthon**	**Separation (Å)**
O1….O7w	2.812	O8w….O11w	2.836
O7w….O8	2.852	O11w….O9	2.896
O2….O8w	2.786	O5….O12w	2.703
O8w….O1	2.701	O12w….O2	2.722

Table S2. H-bonding distances for **1-Tb**.

Hydrogen bonding synthon	**Separation (Å)**	**Hydrogen bonding synthon**	**Separation (Å)**
O2……O14W	2.826	O5……O13W	2.666
O3……O14W	3.014	O6……O16W	2.914
O10……O1W	2.709	O16W……O17W	2.843
O1W……O10W	2.834	O10W……O17W	2.843
O4……O10W	2.836	O4……O10W	2.836
O8……O5W	2.798	O8W……O17W	2.719
O13W……O14W	2.837	O3……O8W	2.762
O11W……O13W	2.849	O4W……O12W	2.721
O2W……O11W	2.901	O4W……O8	2.927
O2……O11W	2.715	O12W……O13W	3.001
O3……O12W	2.708	O4W……O12W	2.721

Table S3. Retention time of the organic products as observed from the gas chromatographic experiments.[a]

Entry	Product	Retention time (Min.)
1	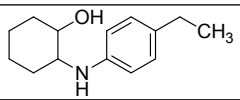	27.0
2	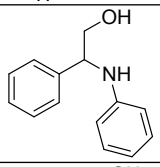	24.2
3	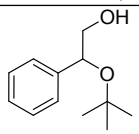	16.6
4	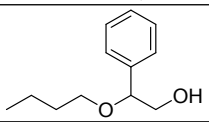	19.7
5	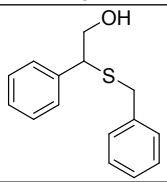	29.2
6	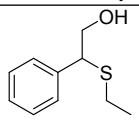	25.7
7	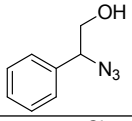	20.8
8	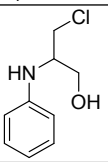	22.8

[a]The products were analyzed by the Perkin Elmer Clarus 580 gas chromatograph equipped with an auto injector, a flame ionization detector and an Elite 5 column (0.25 mm ID, 30 meter). Conditions: nitrogen as the carrier gas with 2 ml/min flow rate; injection volume 1.0 µL; and detector temperature 250 °C. The oven temperature was programmed initially heating at 50 °C for 5 min, followed by heating to 120 °C at 10 °C/min (hold for 5 min), then to 200 °C at 10 °C/min (hold for 5 min) and finally to 300 °C (hold for 3 min) with the total analysis time of ca. 40 min.